The impact of EGR components on ozone decomposition under engine relevant conditions in a rapid compression machine

Yu Song, Fabrice Foucher

The impact of EGR components on ozone decomposition under engine relevant conditions in a Rapid Compression Machine

Y. Song * and F. Foucher

Laboratoire PRISME, Université d'Orléans, Polytech Vinci – 45072 Orléans cedex, France

*yu.song@univ-orleans.fr; fabrice.foucher@univ-orleans.fr

Abstract

In this work, with the addition of 90 ppm ozone, the influence of the main EGR components, namely nitrogen, carbon dioxide, steam, and methane, along with the gasoline surrogate iso-octane, on ozone oxidation were investigated at 30 bar, 800 K using a rapid compression machine (RCM). Taking the case diluted with nitrogen as a reference, it was found that the chemical effects of CO_2 on ozone decomposition accelerated with the increase in the carbon dioxide concentration. The promoting effect of steam on ozone decomposition remained constant regardless of the steam mole fraction added. The mutual effect of methane and ozone was detectable, but the enhancement of ozone decomposition was lower than when iso-octane was added. A comprehensive detailed kinetic model was employed to interpret the experimental data. The model performance was improved by replacing the rate coefficients of $O_3+O=2O_2$. Analysis of the rate of production showed that the $IC_8H_{18}+O=CC_8H_{17}+OH$ reaction predominated over the chain terminating reaction $O_3+O=2O_2$, which can explain the significant promoting effect in the presence of iso-octane. When steam is added, two OH radicals are derived from the chain branching reaction $H_2O+O=2OH$. When methane is added, only one OH radical, originating from the O radical attacking methane, is formed. Consequently, the promoting effect of methane addition is the lowest.

Keywords: Ozone decomposition; EGR components; rapid compression machine.

1. Introduction

Ozone (O_3) is a popular plasma oxidizer which has attracted widespread attention during the last decade. When applied to the combustion field, it exhibits significant advantages in terms of ignition promotion especially in the ultra-lean combustion mode, which can provide better efficiency and attenuate pump losses [1]. The byproducts of ozone decomposition are oxygen atoms (O) and molecular oxygen (O_2), which are very environmentally friendly. The use of ozone-assisted combustion would therefore simultaneously fulfill the two requirements of high efficiency and low emissions. In particular, it could solve the issues associated with on-load vehicle auto-ignition in Homogeneous Charge Compression Ignition (HCCI) engines. Given the fact that commercial ozone generators are compact and economical, ozone-assisted combustion could serve as an alternative method to deal with the ignition process [2].

Reports associated with ozone-assisted combustion can be found in engine studies [1-8], jet-stirred reactors [9-10], flow reactors [11], shock tubes [12-15], and flame studies [16-17]. Among engine studies, the impact of ozone on various kinds of fuels has been investigated, ranging from light alkane (natural gas) [5] to primary reference fuel blends [6], with an extension to alcohol [7]. In general, ozone addition was found to have a promoting effect on fuel activity, apart from one case [8] in which ozone and NO were injected simultaneously, where it delayed iso-octane combustion when the ozone concentration was less than half of the nitric oxide concentration seeded. This is attributed to the reaction between ozone and nitric oxide, yielding nitric dioxide and oxygen. Recently, in our group, Seignour et al. [18] experimentally investigated the effect of different gas compositions, namely exhaust gas recirculation (EGR) components, on ozone decomposition in a diesel engine, since EGR is considered a promising method to overcome emission mitigation issues. However, as temperature stratification may exist inside the engine, a better controlled experimental apparatus relevant to engine studies is necessary to obtain more precise experimental results.

A rapid compression machine (RCM), which operates at low-intermediate temperatures and intermediate-high pressures, is a well-suited for engine relevant studies. Equipped with a well-designed crevice in the piston, an RCM can guarantee temperature homogeneity in the core region since the effect of the boundary layer is negligible. In a recent study on ozone-enhanced compressed ignition in an RCM [19], it was found that ozone decomposition accelerated when the charge temperature was increased, oxygen

concentration was reduced, or fuel was added. In the unfueled condition, the temporal prediction of O_3 decomposition was generally retarded too much by the model adopted. It appears that the impact of the diluent on ozone decomposition is still unclear.

From the modelling point of view, Sun [20] reviewed the kinetic models in terms of O_3 oxidation. Several elementary reactions included in the O_3 sub-mechanism were highlighted. Various kinetic models associated with O_3 oxidation have been put forward to predict the experimental results. In terms of ozone decomposition reactions, early in the 1960s, Benson and Axworthy [21] studied the $O_3+M=O_2+O+M$ reaction, which is an initial step for ozone reactions. This was followed by numerical studies devoted to this elementary reaction [22-25]. In 2013, Peukert et al. [26] experimentally and numerically measured and validated the rate of $O_3+M=O_2+O+M$ with the reflected shock tube technique using O-atom atomic resonance absorption spectrometry (ARAS) detection. Temperature and pressure dependent rate coefficients were proposed in this work, but the third-body role of triatomic molecules such as CO_2 and H_2O was not addressed. On the other hand, the rate constants of the $O_3+O=2O_2$ reaction remain more uncertain; the most common rate constants adopted in the O_3 mechanism are derived from the evaluation by Atkinson et al. [27]. Hence, a validation of the current O_3 kinetic model is needed.

The purpose of this study was to extend previous work [18-19] to an experimental and modelling study aiming to determine the impact of different EGR intermediate species on ozone decomposition with the aid of an RCM setup. A modified comprehensive kinetic model was used to interpret the experimental data. A rate of production (ROP) analysis was also conducted to study the chemical effects of the various additives on ozone decomposition.

2. Experimental setup

The experimental apparatus used in this work was a classical single piston RCM, developed and built by the University of Orléans. A detailed description of this setup can be found in [28]; here, only a brief description is given. Firstly, homogeneity inside the combustion chamber of the RCM is guaranteed thanks to the crevice design, which allows strong absorption of boundary layers. It was therefore assumed that compression in the core area of the chamber was isentropic. With the aid of a mass flow controller, the gases (CH_4, O_2, N_2 and CO_2) from the individual cylinders supplied by Messer (purities of 99.99%) passed through

the manifold and entered the mixture tank (volume of 4.08 L) directly. Liquid iso-octane and deionized water were injected into the tank by the syringe with the desired value. Apart from the gas supply system, the main part of the RCM was equipped with several kinds of temperature and pressure sensors. A type K thermocouple with an accuracy of ± 1 K was used to measure the intake temperature.

An Anseros COM-AD-01 corona-discharge ozone generator was used to generate ozone in the RCM chamber. With the intake bypass connected to the compressed air, the ozone was generated at the outlet of the generator. An ozone analyzer (Anseros Ozomat MP6060) with a range of 0-200 ppm ozone was used to measure and monitor the desired ozone mole fraction.

Two opposed Suprasil windows were mounted on the sides of the RCM chamber head to provide optical access. UV light was produced by an Ocean Optics Deuterium Lamp, and collimated by a lens into a Thorlab integrating sphere. A Hamamatsu photomultiplier tube (254 nm) was employed to collect the signals through the port. A schematic of the setup is shown in Fig.1.

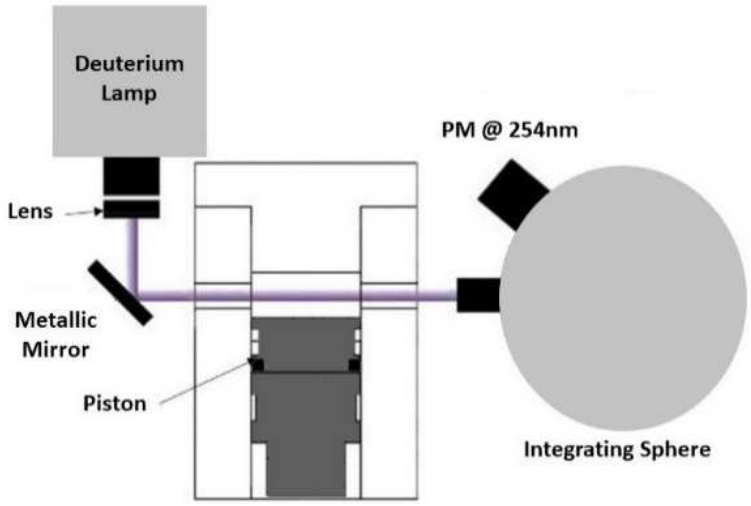

Fig.1. Schematic of optical setup of the RCM. PM: photomultiplier

The signal was recorded and analyzed over 20 shots by the RCM. Two independent samples were measured during each experiment. One is a "reference" sample in which no ozone was injected into the system to account for the light attenuation from the optical setup, and the other is a "target" sample with ozone seeded. The ozone mole fraction was calculated with the Beer-Lambert Law:

$$X_{O3} = \ln\left(\frac{I_{ref}}{I}\right)\frac{K_b T}{PB\sigma_{O3}}$$

where I_{ref} is the reference sample absorption rate, I is the target sample absorption rate, K_b is the Boltzmann constant, B is the bore diameter, σ_{O3} denotes the absorption cross section at 254 nm as a function of temperature [29], T and P are the in-cylinder temperature and pressure, respectively. In-cylinder temperature was deduced from the in-cylinder pressure trace.

3. Kinetic Model

The mechanism adopted in this work consists mainly of the recent comprehensive kinetic model used in [8], in which the ozone decomposition reactions were updated. A modification to the $O_3+M=O_2+O$ reaction was made [30], which turns out to predict the experimental data better. The third body coefficient of triatomic molecules (CO_2 and H_2O) was adopted following the modularity principle behind [21]. The current complete mechanism (1037 species and 4250 reactions) is provided in the supplementary material (SM) in CHEMKIN format, along with thermodynamic properties.

4. Results and discussion

Ozone decomposition measurements were conducted in the presence of various amounts of N_2, CO_2, H_2O, CH_4 and the gasoline surrogate iso-octane in the 313-800 K temperature range and at a pressure of 30 bar. The experimental conditions investigated in this study are presented in Table 1. The initial experimental conditions selected are relevant to engine conditions. Numerical calculations were performed with CHEMKIN-PRO software [31]. A closed homogenous reactor solver with variable volume profiles (see SM), which was derived from the aforementioned non-reactive pressure profiles by adopting the calculation methods proposed in [32], was employed for ozone quantification.

4.1 Experimental results and comparison with simulations

The ozone conversions as a function of time under various conditions are presented in this section. Simulation results are also shown to compare with the experimental data. Experimental results are represented by solid lines, and simulations by different types of dashed lines in all the figures depicted in this part.

4.1.1 Ozone decomposition diluted in nitrogen

Fig.2 shows the ozone (90 ppm) decomposition diluted in nitrogen as a function of time, along with the corresponding temperature and pressure profiles. A small ozone consumption can be observed between t= -5 ms to t=-2 ms, followed by a steep ozone consumption until complete depletion is achieved. Note that the initial oscillation arises from the uncertainty and the vibrations caused by the UV technology and RCM apparatus, respectively.

Table 1 Experimental conditions (Inlet composition volume basis; ozone mole fraction: 90 ppm; End of compression pressure P_c = 30 bar).

Exp.	T_{in} [K]	X_{N2}	X_{O2}	X_{CO2}	X_{H2O}	X_{CH4} [ppm]	X_{IC8H18} [ppm]
1	313	0.79	0.20991	-	-	-	-
2	313	0.395	0.20991	0.395	-	-	-
3	313	0.5925	0.20991	0.1975	-	-	-
4	313	0.69125	0.20991	0.9875	-	-	-
5	333	0.395	0.20991	0.395	-	-	-
6	353	0.5925	0.20991	0.1975	-	-	-
7	393	0.69125	0.20991	0.9875	-	-	-
8	313	0.69	0.20991	-	0.1	-	-
9	313	0.74	0.20991	-	0.05	-	-
10	313	0.765	0.20991	-	0.025	-	-
11	313	0.7895	0.20991	-	-	500	-
12	313	0.78975	0.20991	-	-	250	-
13	313	0.7895	0.20991	-	-	-	500
14	313	0.78975	0.20991	-	-	-	250

Two simulations were compared in this work. First, with the previous model (Model-1) used in [18], a retarding effect was detected compared to the experimental trend. On replacing the rate coefficient of $O_3+O=2O_2$ [30], the prediction improved as the sharp consumption timing was better captured by the updated model (Model-2), although the model still failed to predict the initial slow ozone consumption zone

(t= -5 to -2 ms). Overall, good agreement between the steep ozone oxidation experimental data and model output was observed. A possible explanation for the slow ozone consumption might be the surface effect when the temperature is above 550 K.

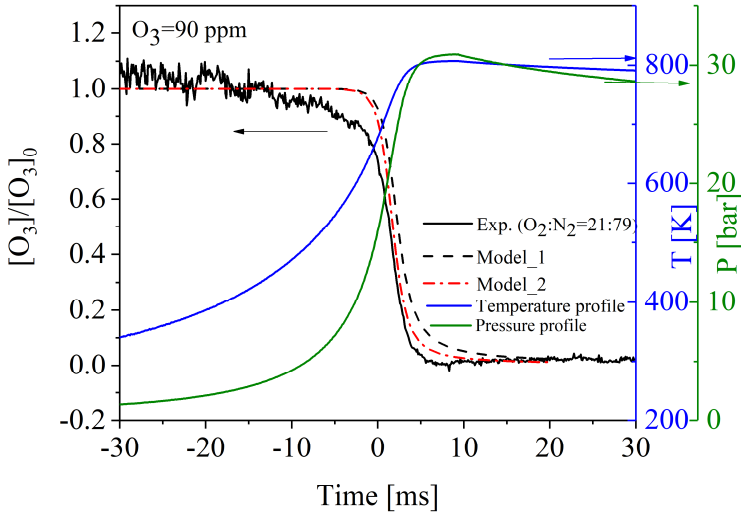

Fig.2 Ozone decomposition as a function of time during the compression stroke. Solid lines denote the experimental results and dashed lines represent the simulation. Temperature and pressure profiles are also provided as a reference.

4.1.2 The impact of carbon dioxide

Fig. 3 shows the ozone decomposition profile with different amounts of carbon dioxide (0, 9.875%, 19.75%, 39.5%) as a function of time. In these cases, the initial temperatures were kept the same (313 K). The end pressures (P_c) was approximately 30 bar, which is consistent with the cases shown in Fig.2. As for the following cases (steam, methane and iso-octane added), the P_c were all kept at 30 bar. The corresponding temperature profiles are given in Fig.4. Overall, CO_2 addition retarded the initiation of ozone decomposition. In the presence of CO_2, the inhibiting effect increased with the increase in the CO_2 mole fraction. In particular, in the case of 39.5% CO_2 addition, 30% of ozone still remained in the system compared to the nearly completed consumption case without CO_2 addition at a time of 9 ms. Due to the high thermal capacity of CO_2, the temperature profiles with CO_2 addition were generally below that without CO_2, as shown in Fig.4. In this case, the retarding effect might be ascribed to the thermal effect of CO_2, which deteriorates the whole system.

157 The model predicted the experimental data well in the case of 9.875% and 19.75% CO_2 addition, but
158 a deviation between the experimental data and simulation was found with 39.5% CO_2 addition. While it
159 might be assumed that the main role of CO_2 in ozone decomposition is participating in the $O_3+M=O_2+O+M$
160 reaction as a third body, the introduction of the third body coefficient did not in fact impact the model
161 behavior significantly. It could be ascribed to the predominantly thermal role of CO_2 in this temperature
162 range.

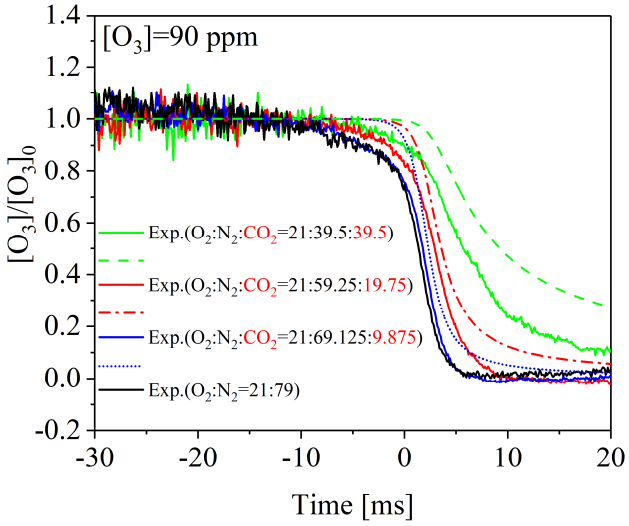

163

164 Fig.3. Ozone decomposition in the presence of CO_2 as a function of time during the compression stroke. Solid
165 lines denote the experimental results and dashed lines represent the simulation.

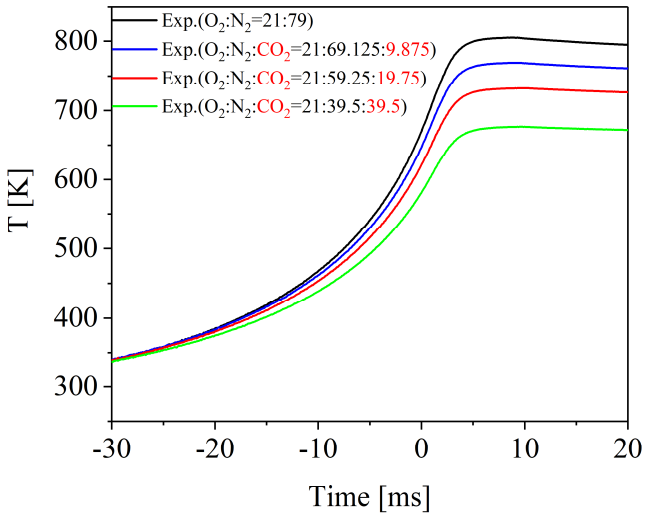

166

Fig.4. The temperature profiles corresponding to the cases shown in Fig.3

In order to decouple the CO_2 thermal effect, another set of experiments was conducted in which the initial temperature was increased to 60, 80, and 120 °C for the three carbon dioxide conditions (9.875%, 19.75%, 39.5%), respectively, to ensure a similar end of compression temperature (T_c). Fig.5 shows the ozone decomposition profile with different amounts of carbon dioxide (0, 9.875%, 19.75%, 39.5%) at a similar end of compression temperature as a function of time. With a similar T_c, the ozone decomposition behavior is dramatically different from those shown in Fig.3. In the case of 9.875% CO_2 addition, ozone decomposition shows a similar trend compared to the one without CO_2 addition, while in the presence of 19.75% CO_2, a slight promoting effect can be observed. As CO_2 is further increased to 39.7%, the accelerating effect becomes significant. Although the temperature profiles for the aforementioned cases are not exactly the same as the one without CO_2 addition as shown in Fig.6, the temperature is consistent among the 0, 9.875%, and 19.75% CO_2 addition cases at t=3 ms. When taking a close look at Fig.5 again at t= 3 ms, one may note that the ozone is consumed more in the presence of CO_2 than without CO_2 addition. This implies that the chemical effect of CO_2 should not be neglected even at 800 K, 30 bar, under engine relevant conditions.

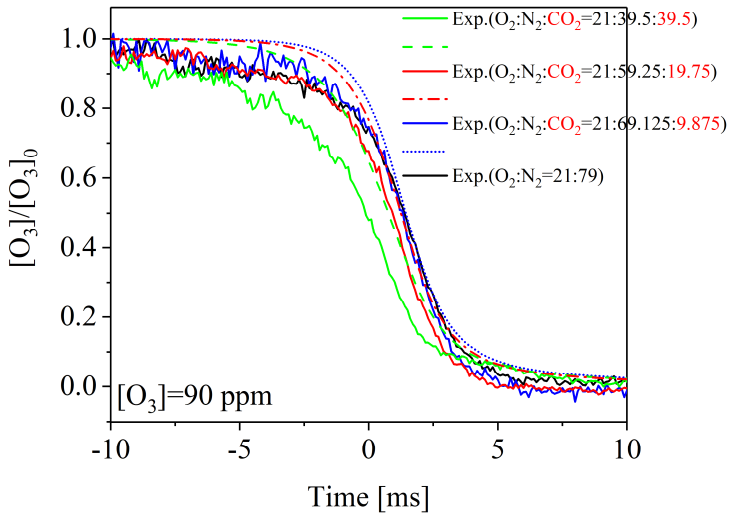

Fig.5. Ozone decomposition in the presence of CO_2 as a function of time during the compression stroke with a similar T_c. Solid lines denote the experimental results and dashed lines represent the simulation.

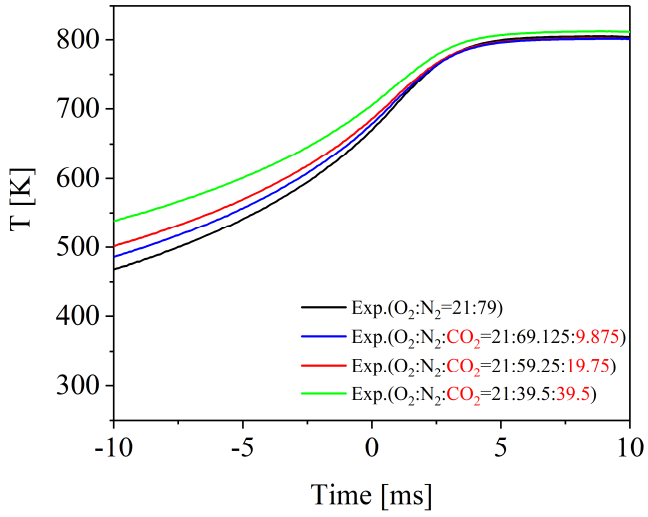

185

186 Fig.6. The temperature profiles corresponding to the conditions shown in Fig.5

187 The model reproduced the cases with different amounts of carbon dioxide (9.875% and 19.75%)
188 reasonably well, but the deviation between the experimental and simulated results became larger when
189 further increasing the carbon dioxide mole fraction to 39.5%. The reason for this poor model performance in
190 the case of a relatively high amount of carbon dioxide is still unclear.

191 4.1.2 The impact of steam

192 Fig.7 shows the ozone decomposition profile with different amounts of steam (0, 2.5%, 5%, 10%) as
193 a function of time. It is interesting to note that different amounts of steam exhibit a very similar promoting
194 trend compared to the one without steam addition, which is also observed in engine work [18]. In addition, at
195 around t= 0.4 ms, a short plateau (1 ms) was observed, after which it continued to decompose. The "plateau"
196 phenomenon could be explained by the potential formation of H_2O_2 or HO_2, which also show characteristic
197 absorption at this wavelength [33]. In general, Fig.7 shows that ozone initiation advances by 2 ms in the
198 presence of steam. In this case, the temperature profiles (Fig.8) are almost the same among all the
199 investigated conditions, except the one with 10% steam addition, whose temperature is 10 K lower. Hence
200 the promoting effects can be attributed to the chemical effect of steam.

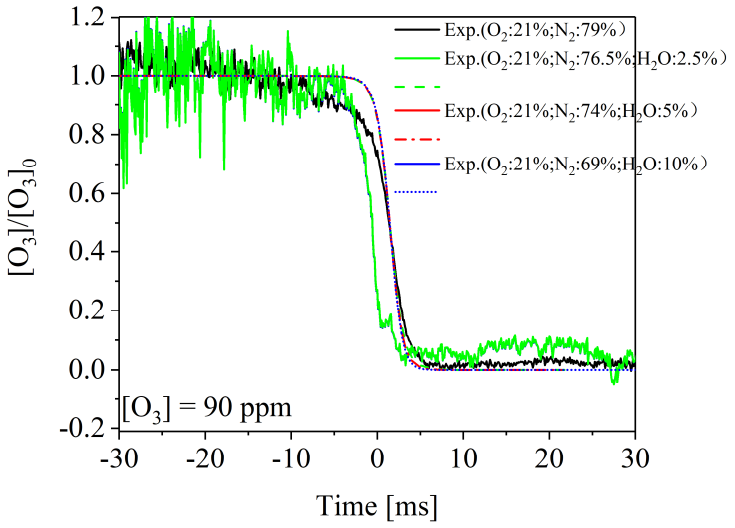

Fig.7. Ozone decomposition in the presence of H_2O as a function of time during the compression stroke. Solid lines denote the experimental results and dashed lines represent the simulation.

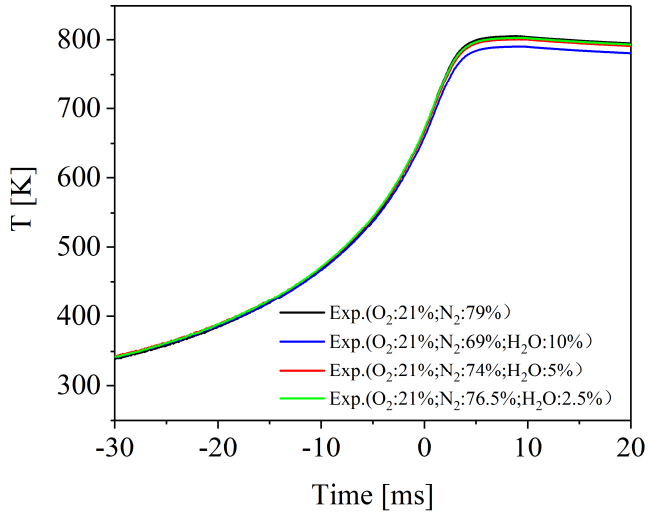

Fig.8. The temperature profiles corresponding to the conditions shown in Fig.7

While the model was able to capture the promoting trend, a retarded model performance was observed compared to the experimental data. A possible explanation for the deviation between the experimental results and numerical calculations could be the inaccuracy of the elementary reaction $O_3+H_2O=H_2O_2+O_2$. Its reaction rate was adopted from the early experimental work by [34]. By implementing this rate constant, the contribution of $O_3+H_2O=H_2O_2+O_2$ is minor as shown in the following analysis (Fig.9).

The rate of production (ROP) analysis (Fig.9 and 10) showed that the main consumption channel for ozone is $O_3+M=O_2+O+M$, following $O_3+O=2O_2$. The ROP of the reaction $O_3+H_2O=H_2O_2+O_2$ was negligible. For steam, $H_2O+O=2OH$ is the main consumption channel; the formation channels are $HO_2+OH=H_2O+O_2$ and $H_2O_2+OH=H_2O+HO_2$. Once ozone has decomposed, the O atoms can react with either ozone or steam. Steam can serve as a promoter since the products of O radicals and steam are hydroxide radicals. On the other hand, $O_3+O=2O_2$ is a chain terminating reaction due to the stable oxygen products. In this case, the participation of steam in the system competes with the chain terminating reaction and yields two OH radicals, which may accelerate ozone decomposition. This could explain the advance of the experimental and model results in the presence of steam shown in Fig.7.

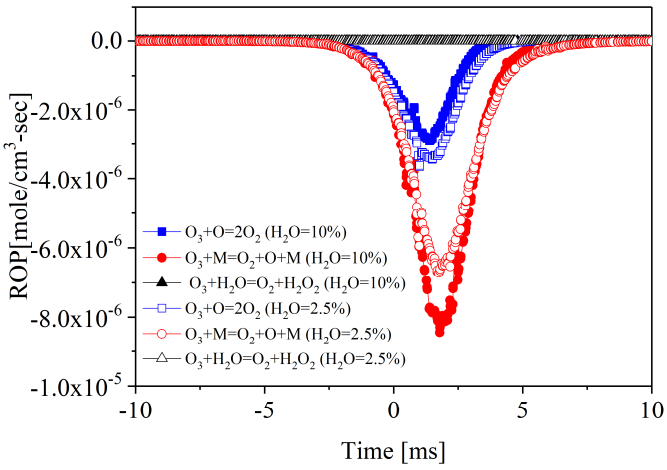

Fig.9. The main rate of production (ROP) involved in ozone as a function of time in the presence of steam

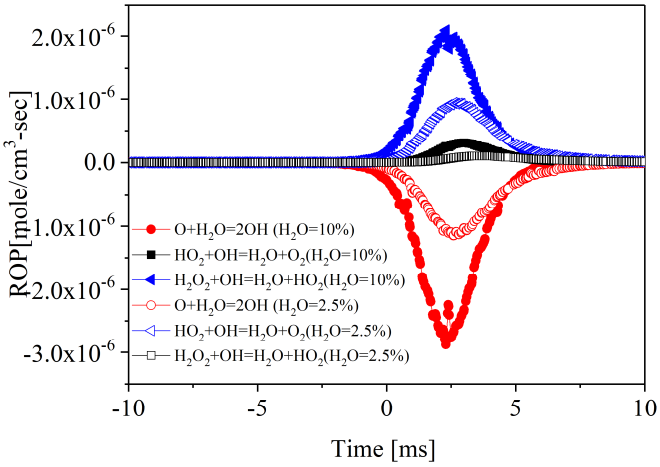

Fig.10. The main rate of production (ROP) involved in steam as a function of time in the presence of steam

It is worth mentioning that different amounts of steam have a very similar promoting trend compared to the case without steam. In [18], the effect of steam was attributed to the low activated energy required by $O_3+H_2O=O_2+O+H_2O$. However, the similar promoting effect in the presence of different amounts of steam was not clarified. In the present work, the ROP involved in steam evolves as shown in Fig.10. The main consumption channel of steam is $H_2O+O=2OH$. The function of this elementary reaction can be twofold: on the one hand, it competes with the chain terminating reaction $O_3+O=2O_2$; on the other hand, the two OH radicals are reactive radicals, which is beneficial to the whole system. It is reported in the review paper [20] that the highly oxidative hydroxy radical attaching ozone is of importance. The main steam formation reactions are OH radical consuming ones, along with the yield of stable products. Note that the ROP of $O_3+H_2O=O_2+O+H_2O$ increases with the increase of steam; accordingly, the ROP of the chain terminating reactions $HO_2+OH=H_2O+O_2$ and $H_2O_2+OH=H_2O+HO_2$ also increase. In sum, the balance of the consumption and formation channels of steam results in the similar influence of various amounts of steam addition on ozone decomposition.

4.1.3 The impact of methane and iso-octane

With methane addition, surprisingly, the accelerating effect was also observed. In [20], it was argued that the interaction between methane and ozone is very limited at room temperature. In contradiction with [20], a promoting effect of methane addition was found here, demonstrating the mutual effect between methane and ozone under engine relevant conditions as shown in Fig.11. In the presence of methane, the acceleration of ozone decomposition was observed after the time (t= 0 ms). Fig.12 shows that the temperature profile was similar with and without methane addition. So the chemical effect of methane is noticeable during the ozone decomposition process.

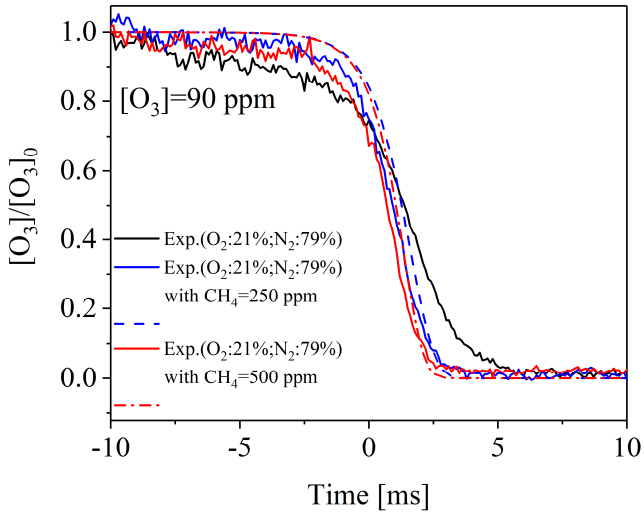

Fig.11. Ozone decomposition in the presence of CH_4 as a function of time during the compression stroke. Solid lines denote the experimental results and dashed lines represent the simulation.

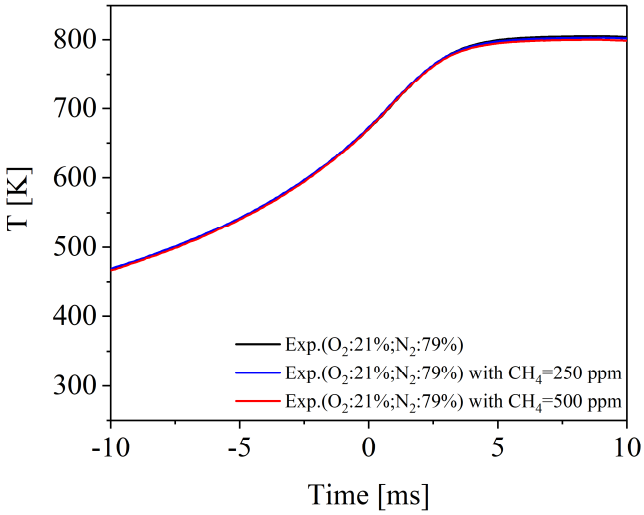

Fig.12. The temperature profiles corresponding to the conditions shown in Fig.11

The agreement between the experimental data and simulation results was generally acceptable although a slight deviation was observed. The promoting effect of methane was also illustrated by ROP analysis. At the beginning of ozone decomposition as shown in Fig.13, $O_3+M=O_2+O+M$ is the main contributing reaction. The chain terminating reaction $O_3+O=2O_2$ also shows a significant effect on ozone decomposition. With regard to methane oxidation (Fig.14), $CH_4+O=CH_3+OH$ exhibits a similar production rate to the $O_3+O=2O_2$ reaction. Only one OH radical is released by the $CH_4+O=CH_3+OH$ reaction. This could explain the relatively small promoting effect compared to the case with steam since two OH radicals

are formed via $H_2O+O=2OH$. On the other hand, $CH_4+OH=CH_3+H_2O$ is the main consumption channel of methane. When comparing the different cases (250 and 500 ppm addition), as shown in Fig.14, it can be seen that the initiation timing of $CH_4+O=CH_3+OH$ with 500 ppm methane addition is advanced compared to the one with 250 ppm addition. Moreover, the more methane is added, the higher the rate of production, which explains the more promoting effect with 500 ppm methane addition.

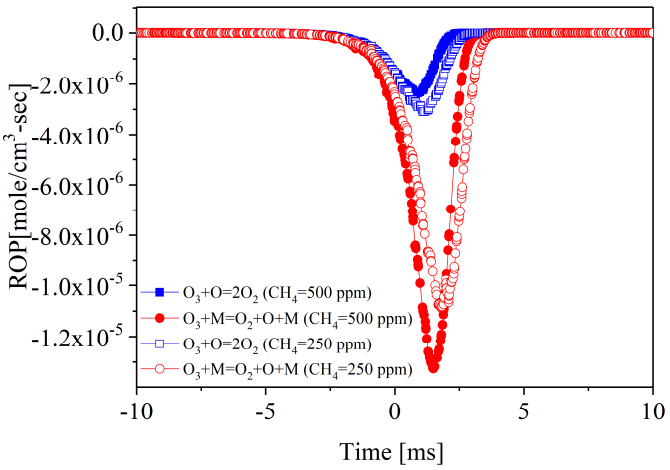

Fig.13. The main rate of production (ROP) involved in ozone as a function of time in the presence of methane

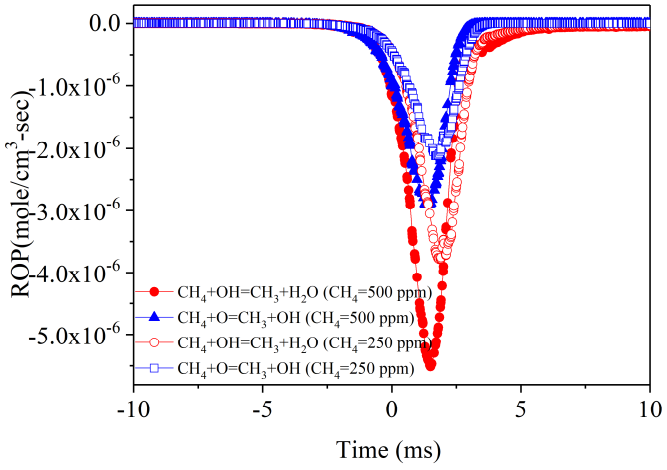

Fig.14. The main rate of production (ROP) involved in methane as a function of time in the presence of methane

The effect of iso-octane addition on ozone decomposition at 30 bar is shown in Fig.15. Two different iso-octane mole fractions (250 and 500 ppm) were tested. As expected, ozone consumption started at early timing, indicating that the presence of iso-octane promotes ozone oxidation. In this case, at around

t=1.4 ms, a small plateau also occurred. However, with the decrease in the iso-octane mole fraction, this plateau vanished. Note that the temperature profile (Fig.16) shows a similar trend when the timing is below 2 ms. This is the timing range of ozone decomposition in the iso-octane addition cases.

The model captured the experimental results well regardless of the prediction failure for the "plateau" characteristic since it is the absorption signal of the HO_2 or H_2O_2 species. The ROP analysis (Fig.17 and 18) showed that the main ozone consumption channel is $O_3+M=O_2+O+M$, while other channels exhibited a minor effect in terms of ozone oxidation. On the other hand, upon the initial iso-octane oxidation, $IC_8H_{18}+O=CC_8H_{17}+OH$ and $IC_8H_{18}+OH=AC_8H_{17}+H_2O$ played a similar role, while the other channels involving $IC_8H_{18}+OH$ exhibited a minor effect compared to that of $IC_8H_{18}+OH=AC_8H_{17}+H_2O$. Note that the yield of O atoms serves as a reactant in the branching reaction $IC_8H_{18}+O=CC_8H_{17}+OH$, as shown in the inset of Fig.18. This reaction plays a dominant role compared to the chain terminating reaction $O_3+O=2O_2$, which shows a small effect on ozone decomposition, as depicted in Fig.17. This is the reason why the promoting effect of iso-octane on ozone decomposition is greater than that of methane. The influence of different amounts of iso-octane on ozone decomposition exhibits the same trend as in the presence of methane.

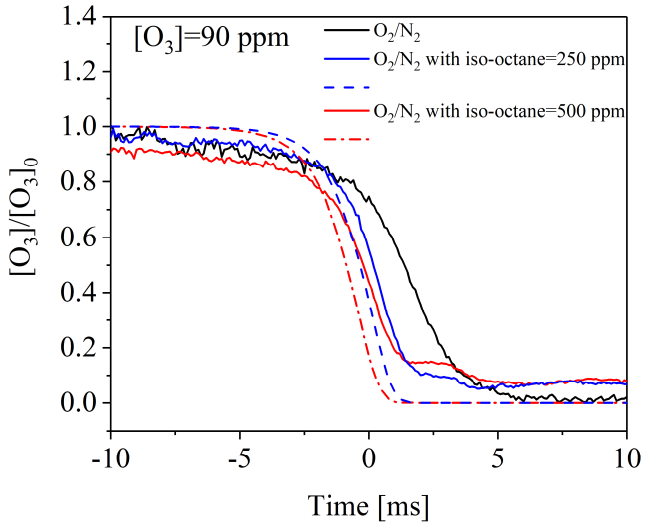

Fig.15. Ozone decomposition in the presence of iso-octane as a function of time during the compression stroke. Solid lines denote the experimental results and dashed lines represent the simulation.

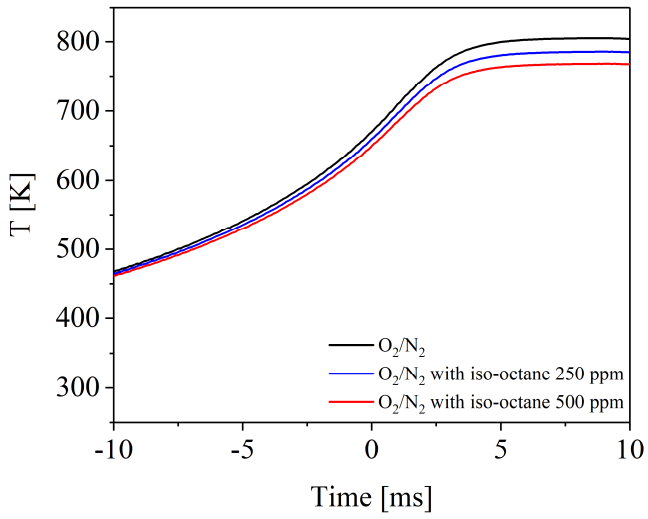

289

290 Fig.16. The temperature profiles corresponding to the conditions shown in Fig.15

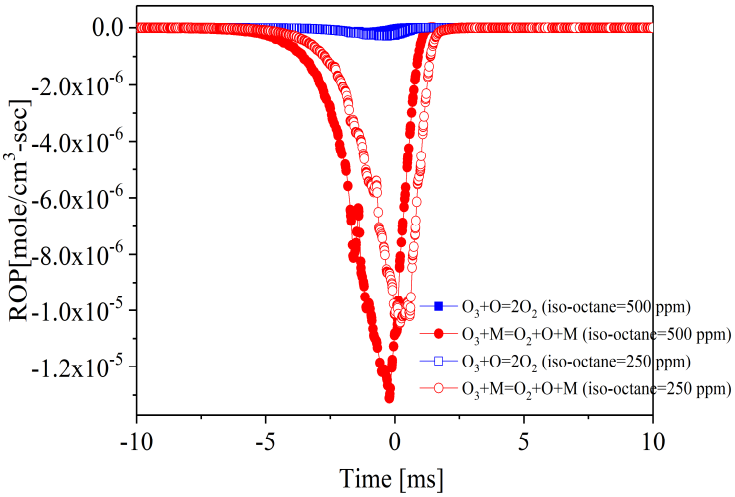

291

292 Fig.17. The main rate of production (ROP) involved in ozone as a function of time in the presence of iso-octane

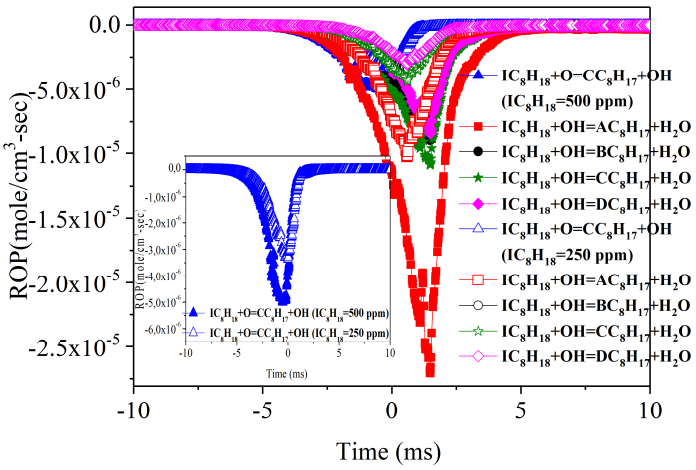

Fig.18. The main rate of production (ROP) involved in iso-octane as a function of time in the presence of iso-octane. The insets present the ROP profile of the IC_8H_{18}+O reaction.

5. Conclusions

In this work, in the presence of 90 ppm ozone, the impact of the main EGR components, i.e. nitrogen, carbon dioxide, steam, and methane along with the gasoline surrogate iso-octane, on ozone oxidation were studied at 30 bar, 800 K with the aid of an RCM. Results reveal that the chemical effect of CO_2 on ozone decomposition increases with the increase in the carbon dioxide mole fraction, whereas the promoting effect of steam on ozone decomposition remains constant regardless of the steam concentration added. The enhancement of ozone decomposition is less in the presence of methane compared to that of iso-octane. A comprehensive detailed kinetic model with rate modification of O_3+O=2O_2 was employed to interpret the experimental data. It is found that the reaction IC_8H_{18}+O=CC_8H_{17}+OH strongly dominates the chain terminating reaction O_3+O=2O_2 in the presence of iso-octane. As for steam additives, the chain branching reaction H_2O+O=2OH shows a high production rate and is of particular importance since it competes with the chain terminating reaction O_3+O=2O_2 and two OH radicals are formed. The ROP of CH_4+O=CH_3+OH is similar to that of O_3+O=2O_2, and only one OH radical is released in the presence of methane.

Acknowledgements

The research leading to these results has received funding from the French Government's Investissement d'Avenir program: Laboratoire d'Excellence CAPRYSSES (Grant No ANR-11- LABX-0006-01).

References

[1] Contino F, Masurier J-B, Foucher F, Lucchini T, D'Errico G, Dagaut P. CFD simulations using the TDAC method to model iso-octane combustion for a large range of ozone seeding and temperature conditions in a single cylinder HCCI engine. Fuel. 2014;137:179-84.

[2]Masurier J-B, Foucher F, Dayma G, Rousselle C, Dagaut P. Application of an Ozone Generator to Control the Homogeneous Charge Compression Ignition Combustion Process. SAE International; 2015.

[3] Kobashi Y, Wang Y, Shibata G, Ogawa H, Naganuma K. Ignition control in a gasoline compression ignition engine with ozone addition combined with a two-stage direct-injection strategy. Fuel. 2019;249:154-60.

[4] Schönborn A, Hellier P, Aliev AE, Ladommatos N. Ignition control of homogeneous-charge compression ignition (HCCI) combustion through adaptation of the fuel molecular structure by reaction with ozone. Fuel. 2010;89:3178-84.

[5] Masurier J-B, Foucher F, Dayma G, Dagaut P. Effect of Additives on Combustion Characteristics of a Natural Gas Fueled HCCI Engine. SAE International; 2014.

[6] Foucher F, Higelin P, Mounaïm-Rousselle C, Dagaut P. Influence of ozone on the combustion of n-heptane in a HCCI engine. Proceedings of the Combustion Institute. 2013;34:3005-12.

[7] Masurier JB, Foucher F, Dayma G, Dagaut P. Ozone applied to the homogeneous charge compression ignition engine to control alcohol fuels combustion. Applied Energy. 2015;160:566-80.

[8] Masurier J-B, Foucher F, Dayma G, Dagaut P. Investigation of iso-octane combustion in a homogeneous charge compression ignition engine seeded by ozone, nitric oxide and nitrogen dioxide. Proceedings of the Combustion Institute. 2015;35:3125-32

[9] Rousso AC, Hansen N, Jasper AW, Ju Y. Low-Temperature Oxidation of Ethylene by Ozone in a Jet-Stirred Reactor. J Phys Chem A. 2018;122:8674-85.

[10] Rousso AC, Hansen N, Jasper AW, Ju Y. Identification of the Criegee intermediate reaction network in ethylene ozonolysis: impact on energy conversion strategies and atmospheric chemistry. Phys Chem Chem Phys. 2019;21:7341-57.

[11] Zhao H, Yang X, Ju Y. Kinetic studies of ozone assisted low temperature oxidation of dimethyl ether in a flow reactor using molecular-beam mass spectrometry. Combustion and Flame. 2016;173:187-94.

[12] Jones WM, Davidson N. The thermal decomposition of ozone in a shock tube. Journal of the American Chemical Society. 1962;84:2868-78.

[13] Heimerl JM, Coffee TP. The unimolecular ozone decomposition reaction. Combustion and Flame. 1979;35:117-23.

[14] Michael J. Thermal decomposition of ozone. The Journal of Chemical Physics. 1971;54:4455-9.

[15] Peukert SL, Sivaramakrishnan R, Michael JV. High Temperature Shock Tube Studies on the Thermal Decomposition of O3 and the Reaction of Dimethyl Carbonate with O-Atoms. J Phys Chem A. 2013;117:3729-38.

[16] Ombrello T, Won SH, Ju Y, Williams S. Flame propagation enhancement by plasma excitation of oxygen. Part I: Effects of O3. Combustion and flame. 2010;157:1906-15..

[17] Zhang Y, Zhu M, Zhang Z, Shang R, Zhang D. Ozone effect on the flammability limit and near-limit combustion of syngas/air flames with N2, CO2, and H2O dilutions. Fuel. 2016;186:414-21.

[18] Seignour N, Khacef A, Foucher F. Experimental Understanding of Ozone Decomposition inside a Low-Temperature Combustion Engine. Combustion Science and Technology. 2019:1-12.

[19] Seignour N, Ekoto I, Foucher F, Moreau B. Measurements and modeling of ozone enhanced compression ignition in a rapid compression machine and optically-accessible engine. SAE International; 2019.

[20] Sun W, Gao X, Wu B, Ombrello T. The effect of ozone addition on combustion: Kinetics and dynamics. Progress in Energy and Combustion Science. 2019;73:1-25.

[21] Benson SW, Axworthy Jr AE. Mechanism of the gas phase, thermal decomposition of ozone. The Journal of Chemical Physics. 1957;26:1718-26.

[22] Jones WM, Davidson N. The thermal decomposition of ozone in a shock tube. Journal of the American Chemical Society. 1962;84:2868-78.

[23] Michael J. Thermal decomposition of ozone. The Journal of Chemical Physics. 1971;54:4455-9.

[24] Heimerl JM, Coffee TP. The unimolecular ozone decomposition reaction. Combustion and Flame. 1979;35:117-23.

[25] Thoma M, Hindelang F. Experiments on shock-heated ozone dissociation in oxygen/air using UV laser spectroscopy. Shock Waves@ Marseille II: Springer; 1995. p. 59-64.

[26] Peukert SL, Sivaramakrishnan R, Michael JV. High Temperature Shock Tube Studies on the Thermal Decomposition of O3 and the Reaction of Dimethyl Carbonate with O-Atoms. J Phys Chem A. 2013;117:3729-38.

[27] Atkinson R, Baulch D, Cox R, Crowley J, Hampson R, Hynes R, et al. Evaluated kinetic and photochemical data for atmospheric chemistry: Volume I-gas phase reactions of Ox, HOx, NOx and SOx species. Atmospheric chemistry and physics. 2004;4:1461-738.

[28] M. Pochet, V. Dias, B. Moreau, F. Foucher, H. Jeanmart, F. Contino, Experimental and numerical study, under LTC conditions, of ammonia ignition delay with and without hydrogen addition, *Proc. Combust. Inst.*, 37 (2019) 621-629.

[29] D.C. Astholz, A.E. Croce, J. Troe, Temperature Dependence of the Ozone Absorption Coefficient in the Hartley, J. Phys. Chem. 86 (1982), 696-699.

[30] Arnold I, Comes F. Temperature dependence of the reactions O (3P)+ O3→ 2O2 and O (3P)+ O2+ M→ O3+ M. Chemical Physics. 1979;42:231-9.

[31] CHEMKIN-PRO 15083, Reaction Design, San Diego, (2013)

[32] G. Mittal, M. Raju, C.-J. Sung, Computational fluid dynamics modeling of hydrogen ignition in a rapid compression machine, *Combust. Flame*, 155 (2008) 417-428.

[33] Moortgat G, Veyret B, Lesclaux R. Absorption spectrum and kinetics of reactions of the acetylperoxy radical. The Journal of Physical Chemistry. 1989;93:2362-8.

[34] Hatakeyama S, Leu MT. Rate constants for reactions between atmospheric reservoir species. 2. Water. The Journal of Physical Chemistry. 1989;93:5784-9.